Lawrence Berkeley National Laboratory
Recent Work

Title
Decay Studies of Neutron Deficient Nuclei near the Z

Permalink
https://escholarship.org/uc/item/06w0g25v

Journal
Physical review C, 43(3)

Authors
Firestone, R.B.
Gilat, J.
Nitschke, J.M.
et al.

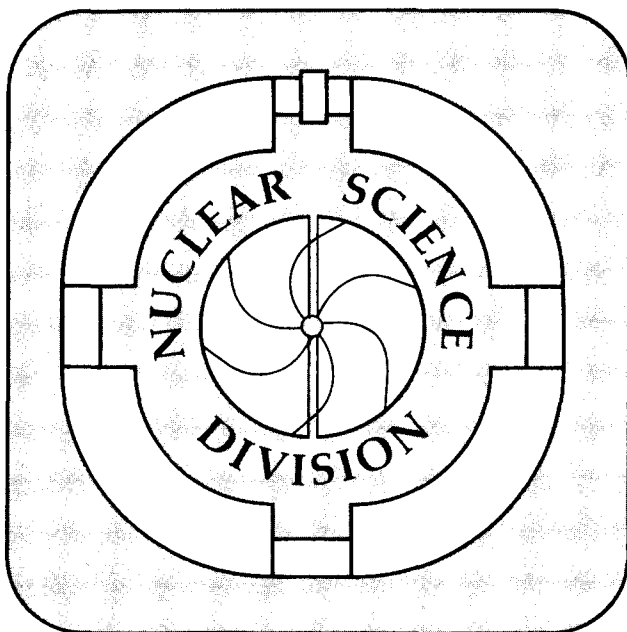**Publication Date**
1990-09-01

Lawrence Berkeley Laboratory
UNIVERSITY OF CALIFORNIA

Decay Studies of Neutron Deficient Nuclei near the Z=64 Subshell: ^{142}Dy, ^{140,142}Tb, ^{140,142}Gd, ^{140,142}Eu, ^{142}Sm and ^{142}Pm

R.B. Firestone, J. Gilat, J.M. Nitschke,
P.A. Wilmarth, and K.S. Vierinen

September 1990

NUCLEAR SCIENCE DIVISION

DISCLAIMER

Decay Studies of Neutron Deficient Nuclei Near the Z=64 subshell:
^{142}Dy, ^{140,142}Tb, ^{140,142}Gd, ^{140,142}Eu, ^{142}Sm and ^{142}Pm

R.B. Firestone, J. Gilat, J.M. Nitschke, P.A. Wilmarth, and K.S. Vierinen
Lawrence Berkeley Laboratory
University of California, Berkeley, California 94720, USA

September 1990

Decay studies of neutron deficient nuclei near the Z=64 subshell:

^{142}Dy, ^{140,142}Tb, ^{140,142}Gd, ^{140,142}Eu, ^{142}Sm and ^{142}Pm

R. B. Firestone, J. Gilat[†], J. M. Nitschke, P. A. Wilmarth, and K. S. Vierinen[*]

Lawrence Berkeley Laboratory, Berkeley, California 94720

The EC/β^+ and delayed proton decays of A=142 isotopes with $61 \le Z \le 66$ and A=140 isotopes with $63 \le Z \le 65$ were investigated with the OASIS facility on-line at the LBL SuperHILAC. Electron capture and positron decay emission probabilities have been determined for ^{142}Pm and ^{142}Sm decays, and extensive decay schemes have been constructed for ^{142}Eu^g(2.34±0.12 s), ^{142}Gd(70.2±0.6 s), ^{140}Eu(1.51±0.02 s), and ^{140}Gd(15.8±0.4 s). Decay schemes for the new isotopes ^{142}Tb^g(597±17 ms), ^{142}Tb^m(303±17 ms), ^{142}Dy(2.3±0.3 s), ^{140}Eu^m(125±2 ms), and ^{140}Tb(2.4±0.2 s) are also presented. We have assigned γ rays to these isotopes on the basis of $\gamma\gamma$- and xγ-coincidences, and from half-life determinations. Electron capture and β^+ decay branchings were measured for each decay, and β-delayed proton branchings were determined for ^{142}Dy, ^{142}Tb and ^{140}Tb decays. Q_{EC} values, derived from the measured EC/β^+ branchings and the level schemes are compared with those from the Wapstra and Audi mass evaluation and the Liran and Zeldes mass calculation. The systematics of the N=77 isomer decays are discussed, and the intense $0^+ \rightarrow 1^+$ and $1^+ \rightarrow 0^+$ ground state beta decays are compared with shell model predictions for simple spin-flip transitions.

[†]*Soreq Nuclear Research Center, Yavne 70600, Israel*

[*]Present address: *University of Helsinki, SF-00170, Helsinki, Finland*

I. INTRODUCTION

This paper continues our studies of light rare-earth nuclei with N≤82. Here we report the results of our investigation of the radioactive decays of the neutron deficient nuclei ^{142}Dy, ^{142}Tb^{g+m}, ^{140}Tb, ^{142}Gd, ^{142}Eu^g, ^{140}Eu^{g+m}, ^{142}Sm, and ^{142}Pm. We have previously reported preliminary results for ^{142}Dy, ^{142}Tb^{g+m}, ^{140}Tb, ^{140}Gd, and ^{140}Eu^m decays.[1,2] The decay schemes for ^{142}Sm and ^{142}Pm were already well studied and are summarized by Peker.[3] We remeasured the β-emission probabilities for these decays and determined their total electron capture and β$^+$ branchings. The decay of ^{142}Eu^g was investigated initially by Habs et al.[4] and by Kennedy et al.[5] We have placed additional transitions in the ^{142}Eu^g decay scheme and determined new γ-ray and β-emission probabilities. The decay of ^{142}Gd was first investigated by Habs et al.[6] and later a partial decay scheme was constructed by Turcotte et al.[7] In this paper, we present a more extensive decay scheme for ^{142}Gd with absolute γ-ray and β-emission probabilities. The decay of ^{140}Eu^g was first reported by Westgaard,[8] and a decay scheme was constructed by Beraud et al.[9] We present a more comprehensive picture of the decay of this isotope and a decay scheme for the 125 msec isomer ^{140}Eu^m. The isotope ^{140}Gd was first reported by Redon et al.[10] A 20 sec activity identified by Habs et al.[6] in 1972 as an isomer of ^{140}Eu was probably due to ^{140}Gd. Partial ^{140}Gd decay schemes were prepared by Beraud et al.[9] and by Turcotte et al.[11] We present a more extensive decay scheme with absolute γ-ray and β-emission probabilities. No data other than our previously reported preliminary results,[1,2] could be found in the literature regarding the decay of ^{140,142}Tb and of ^{142}Dy.

We have measured total electron capture and β$^+$ branchings for all the aforementioned decays. From the decay schemes and the measured EC/β$^+$ branchings, we have derived Q$_{EC}$ values which agree well with both the evaluated values of Wapstra et al.[12] and the calculated values of Liran and Zeldes.[13]

II. EXPERIMENTAL METHODS

Sources of above isotopes were produced by ^{92}Mo(HI,xpyn) reactions with 261 MeV ^{54}Fe and 224 MeV

[52]Cr (for A=142) and 312 MeV [54]Fe and 244 MeV [52]Cr (for A=140) ions accelerated at the Lawrence

Berkeley Laboratory SuperHILAC. Products recoiling from the [92]Mo metal foil target (97% enriched)

were mass separated with the OASIS on-line facility,[14] collected on a programmable moving tape, and

transported to a shielded detector array consisting of a Si particle ΔE-E telescope and a hyperpure Ge

detector facing the radioactive source, and of a 1-mm thick plastic scintillator and an n-type Ge detector on

the other side of the collector tape. An additional n-type Ge detector oriented at 90° with respect to the two

other Ge detectors was located ~4.5 cm from the source. A schematic view of the detector arrangement is

shown in Fig.1. In the experiments with [54]Fe beams, 8 s and 400 s (for A=142) and 8 s and 80 s (for

A=140) tape cycles were used and the close-in n-type Ge had 24% efficiency while the 90° detector had

52% efficiency. For the [52]Cr experiments, the tape cycles were 2.4 s and 1.6 s, and the two n-type detec-

tors were interchanged. Coincidences between particles, γ rays, x rays, and positrons were recorded in an

event-by-event mode; all events were tagged with a time signal for half-life information. Singles spectra

were taken with the close-in detector in a multispectrum mode in which the tape cycle time was divided

into eight equal-time counting intervals. During the 2.4-s cycle for A=142 and the 1.6-s cycle for A=140,

singles spectra were also taken in the 90° detector which was less subject to summing than the the close-in

52% detector. The detectors were calibrated for absolute efficiency with commercial standard sources.

Relative intensities and energies were calibrated with sources of [66]Ga, [152]Eu, [226]Ra, and [241]Am. Analysis

of the singles data was performed with the computer code SAMPO[16] and coincidence data were analyzed

using software described in Refs. 17-19. Further experimental details may be found in Refs. 14 and 15.

III. EXPERIMENTAL RESULTS AND ANALYSIS

A. Gamma ray data

Transitions were assigned to the individual A=142 and A=140 activities on the basis of γγ and xγ coin-

cidences, and by half-life analysis. The coincidence results are summarized in Tables I and II. Multipolar-

ities were adopted from published values except for transitions in the decays of ^{142}Dy, ^{142}Tb^{g+m} and ^{142}Eu^m which were analyzed on the basis of coincidence information and decay scheme intensity balances. For some transitions, which were only observed in coincidence data, approximate γ-ray intensities were derived from the data.

B. Decay scheme normalization

An absolute normalization of the transition intensities is required to calculate the β-decay intensity populating the ground state and isomeric states in the daughter. Determination of electron capture and β^+ branching ratios can also help distinguish between ground-state feedings (β^+ dominated) and unobserved decay to high-lying levels (electron capture dominated) in the daughter.

We determined the electron-capture decay branching for each A=142 isotope and for ^{140}Eu^g and ^{140}Gd decays from K x-ray intensities measured in the hyperpure Ge detector. The group of four K x-ray peaks for each element was analyzed using SAMPO,[16] and good agreement was obtained with relative x-ray intensities in the *Table of Isotopes*.[20] These results are summarized in Table III. The total electron capture intensities were calculated from the K x-ray intensities after corrections for detector efficiency, fluorescence yield,[21] internal conversion, and theoretical EC(K)/EC(total) branchings.[22] The internal conversion contribution was calculated from the measured γ-ray intensities assuming that unmeasured multipolarities were either M1 or consistent with the spin change in the proposed level scheme. A 50% uncertainty was assumed for the unmeasured conversion coefficients. For the A=142 isotopes discussed here, corrections to the K x-ray intensity from internal conversion were generally small.

The relative β^+-decay intensity was calculated from the 511.0-keV annihilation radiation intensity. This intensity was corrected for annihilation-in-flight[23] and apportioned to the various isotopes by a multilinear analysis of the multispectrum γ-ray data. For this analysis, the annihilation intensity associated with the ith isotope is assumed to be proportional to the intensity $I_i(\gamma)$ of a given γ ray from that decay. The total

annihilation intensity thus becomes

$$I(\gamma^{\pm}) = \sum_{i=1}^{n} x_i I_i(\gamma) \tag{1}$$

where x_i are the proportionality constants for the n contributing β^+-emitting isotopes. The γ-ray intensity

data from the various tape cycle experiments were analyzed simultaneously using the IMSL library subroutine RLMUL[24] to obtain the best fit to the values of the parameter set x_i. This method is superior to a standard multi-component half-life analysis because data from different experiments can be combined, in one analysis, without concern for the complex genetic relationships between the members of the mass chain. A significant source of uncertainty in this method was that not all positrons were constrained to annihilate near the source. This resulted in some loss of detection efficiency which we measured as 20(10)% based on the positron intensity observed in the plastic detector.

The total electron capture and β^+ intensities for the A=142 and A=140 isotopes are shown in Table IV. The half-life relationships in the A=142 isobaric mass chain are fortuitous because $^{142}Dy \rightarrow ^{142}Tb$, $^{142}Gd \rightarrow ^{142}Eu^g$, and $^{142}Sm \rightarrow ^{142}Pm$ each form equilibrium pairs which can be followed in appropriate tape-cycle times. $^{140}Gd \rightarrow ^{140}Eu^g$ likewise form an equilibrium pair. At equilibrium, the ratio of γ-ray intensities for transitions from each isotope must be consistent with the normalizations determined from the x-ray and 511-keV data. The absolute transition intensities obtained from the two methods are also shown and compared in Table IV.

C. Determination of Q_{EC}

Values of the total β decay energies Q_{EC} were derived from the decay schemes and the measured total electron capture and β^+ intensities. Assuming a Q_{EC} value and allowed β decay, theoretical EC and β^+ intensities were calculated[22] for each β branch in a given decay scheme. The sum of these intensities were then compared with the experimental values and Q_{EC} was varied until the best agreement was obtained. With

this method, any decay to unobserved high-lying daughter levels will lead to a systematic underestimate of Q_{EC}. Strictly speaking, the values given below should therefore be construed as lower limits. Table V lists the Q_{EC} values derived from our data and compares them with the systematic evaluation of Wapstra and Audi[12] and with calculated values from Liran and Zeldes.[13] The error margins shown for the experimental values represent statistical errors in the measurement of γ-ray intensities and do not include decay scheme uncertainties and other systematic effects. The overall agreement is very good and lends support to both the reliability of the above method for determining Q_{EC} and the completeness of the decay schemes. As a check of unobserved transitions, we used the decay schemes to calculate the relative intensities of K x-rays expected to be in coincidence with the 191.2-kev transition in ^{140}Eu and with the 531.0-kev γ-ray in ^{140}Sm, and compared them with measured values. The agreement is quite gratifying; the K/(EC+β) ratios are: 0.052 (decay scheme) versus 0.049(5) (experiment) and 0.38 (decay scheme) versus 0.39(4) (experiment) for the two γ-rays, respectively. This indicates that the fraction of missing activity is quite low, at least for ^{140}Gd and ^{140}Eu decays. The magnitude of the missing transitions effect can also be estimated by repeating the procedure with a uniformly distributed beta strength with an average logft=5 per MeV of excitation energy in the daughter (compatible with allowed beta strength systematics in this region) added to the region above the experimental decay scheme. The difference between the decay scheme value and the added beta strength value depends on Q_{EC}. Around 4-5 MeV, the difference is only 100-200 keV, well within the margins of error; around 7 MeV it increases to about 200-500 keV, and becomes as large as 1-2 MeV for Q_{EC} values of 9-10 MeV.

D. Determination of β-delayed proton branchings

In A=142, β-delayed protons were observed in the Si particle ΔE-E telescope in coincidence with both Tb and Gd K x-rays. The proton decay data were also consistent with two half-life components of about 0.6 s and 2 s and are therefore presumed to follow the decay of the ^{142}Tb^g and ^{142}Dy precursors.[25] Protons from the 2.4-s tape cycle data (146 events) and the 8-s data (115 events) were divided among the two precursors

with the aid of multicomponent decay analysis using the precursor half-lives determined from the $\beta\gamma$ data, and of coincident x-ray intensities. From the delayed proton intensity and the measured EC and β^+ intensities, we determined a $2.2(11)\times10^{-5}$ β-delayed proton branch for ^{142}Tb^g decay and a $6(3)\times10^{-4}$ branch for ^{142}Dy decay. In A=140, β-delayed proton emission in coincidence with Gd K_α and K_β x-rays was observed. The proton half-life of 2.0(5)s is consistent with the decay of ^{140}Tb. Comparing the proton intensity to the intensity of the 328.4 keV γ transition (assuming all decay intensity deexcites through the $2^+\rightarrow0^+$ transition), we determined a $2.6(1.3)\times10^{-3}$ β-delayed proton branch in ^{140}Tb decay.

In Table VI we compare our experimental delayed proton branches with calculated values obtained from a statistical model using beta strength functions based on a QRPA model of Krumlinde and Moller.[26] Calculated half-lives based on the same beta strength functions are also shown. Details of the calculations can be found in Ref. 25, and will not be elaborated here. For ^{142}Dy and ^{140}Tb precursors the agreement between the experimental and the calculated values of both half-lives and branches is very good. For ^{142}Tb a substantial discrepancy is observed in both parameters (for a discussion of this effect see Sec. V. Conclusions).

IV. DECAY SCHEMES

A. ^{142}Sm and ^{142}Pm

The half-lives of ^{142}Sm and ^{142}Pm were too long to confirm in these experiments. No γ rays could be attributed to the decay of ^{142}Sm, and the transitions reported by Dewanjee et al.[27] could not be confirmed. We produced ^{142}Sm in equilibrium with ^{142}Pm in the 400-s dwell time experiment. From the equilibrium Pm and Sm K x-ray intensities and the total 511-keV annihilation intensity at equilibrium, we determined that ^{142}Sm decays with less than 5% positron emission. Analysis of the equilibrium ^{142}Pm data yielded a relative positron decay branching intensity of 0.771 ± 0.027 which is in good agreement with the value of 0.779 derived by Peker.[3] We also determined an 0.0196 ± 0.0011 branching intensity for the 1576.1-keV γ ray

from ^{142}Pm which differs appreciably from the 0.033 decay branch derived by Peker.[3]

B. ^{142}Eu^g

With the target-projectile combinations used in our experiments, ^{142}Eu could only be produced by the decay of ^{142}Gd, and not directly in the reaction. This allowed us to investigate the ^{142}Eu^g decay without interference from the decay of the 1.22 min isomer ^{142}Eu^m.[5] Due to its lower ionization potential, the ^{142}Eu^g is partially separated in the mass separator ion source from its parent ^{140}Gd, thus allowing the determination of its half-life. The 768.1-keV $2^+ \to 0^+$ transition in ^{142}Sm exhibits a two component decay curve, corresponding to equilibrium with ^{142}Gd and to excess ^{142}Eu emitted directly from the ion source. Assuming the adopted ^{142}Gd half-life of 70.2(6) s (section IV.C), we determined, from a two-component fit, that $t_{1/2}$=2.34(12) s for ^{142}Eu^g. This value is in good agreement with 2.4(2) s measured by Kennedy et al.[5] We have assigned 14 γ-ray transitions to the decay of ^{142}Eu^g. The γ-ray energies and relative intensities are given in Table VII, where they are compared with the intensities of Kennedy et al.[5] Our intensities agree marginally with those of Ref. 5 and we have added six new γ rays. In addition, we propose a tentative E0 transition deexciting the 1451.1-keV level. This transition has not been observed directly but is inferred from excess Sm K x-ray intensity in coincidence with the Sm K x-rays from electron capture. Internal conversion is very weak in ^{142}Eu^g decay and the coincident x-ray intensity is about 4 times as strong as expected. This is consistent with the behavior of the first-excited 0^+ levels in ^{142}Nd and ^{144}Sm[19] where E0 decay branchings have been reported. It is also possible that some of the excess coincident x-ray intensity is due to additional, higher-energy E0 transitions. The decay scheme for ^{142}Eu^g is shown in Fig. 2. Firm (no parentheses) spin and parity assignments are based on (p,t) reaction measurements.[28] We determined $I(\beta^+)/I_\gamma(768)$=8.8(6) in agreement with 8.4(11) from Ref. 5. The excited states of unknown spin and parity fall into two categories. Those levels which deexcite to the ground state are most likely 2^+ since low-lying 1^+ levels are not normally observed in rare-earth even-even nuclei. Levels which deexcite only through the

768.1-keV 2^+ state are probably 0^+ states because ground-state γ-ray feeding from 0^+ levels would be forbidden; no transitions to the ground-state could be associated with the proposed 0^+ states.

C. ^{142}Gd

We have assigned 69 γ-ray transitions to the decay of ^{142}Gd. The γ-ray energies and intensities are summarized in Table VIII where they are compared with values of Turcotte et al.[7] The energy agreements are excellent, however many of our intensities differ significantly. We believe that this is partly because our sources were mass separated while those of Turcotte et al.[7] were not and contained many contaminants. Fig. 3 shows the spectrum of γ rays coincident with Eu K x-rays. From the decay of the most intense γ rays observed in the 400 s dwell time experiment, we determined $t_{1/2}$=70.2(6) s which agrees, within experimental uncertainty, with 69.1(10) s measured by Turcotte et al.[7] The decay scheme for ^{142}Gd decay is given in Fig. 4. It is similar to that in Ref. 7 except that we have identified 12 additional levels and placed 28 additional transitions. The multipolarities in Fig. 4 are from the conversion electron data of Turcotte et al.[7] Assuming no significant, unobserved decay to excited states, the ground state β-branch is 52(2)%. This agrees with the experimental value of 61(33)% by Turcotte et al.,[7] but not with their adopted value of 94%. The latter value was deduced from the apparent first-forbidden unique feeding of the 178.9-keV level. We observe no net feeding to that level, indicating that our decay scheme is more complete and that this β-transition cannot be used for intensity normalization.

D. ^{142}Tb^g

We have assigned 18 γ rays to the decay of ^{142}Tb^g. The γ-ray energies and intensities are summarized in Table IX. Several transitions, observed only in the 2.4-s dwell time, were assigned to ^{142}Tb^g decay and placed in the level scheme by energy sums and differences. Fig. 5 shows a spectrum of γ rays in coincidence with Gd K x-rays. The decay scheme for ^{142}Tb^g is shown in Fig. 6. The 465-keV transition was

observed "in coincidence with itself" and placed twice in the decay scheme. Its intensity was divided on the basis of the coincidence data. The intense 515.3-keV transition (resolved from the 511-keV annihilation peak using SAMPO[16]) was analyzed as a two-component parent-daughter decay to extract a 597(17) ms half-life for ^{142}Tb^g decay. The ^{142}Tb^g parent spin is uniquely determined as 1$^+$ by the low logft value for decay to the 0$^+$ ground state of ^{142}Gd. The lowest 0$^+$, 2$^+$, and 4$^+$ states in ^{142}Gd are known from in-beam spectroscopy.[29,30] The 693.7 keV 4$^+$→2$^+$ is clearly seen, although no transitions were observed populating the 4$^+$ level, and we presume that this level is fed by weak E2 transitions from higher-lying 2$^+$ levels.

E. ^{142}Tb^m isomeric decay

At A=142, the Tb K x-rays, 181.9- and 211.6-keV γ rays were observed to decay with a 303(7) ms half-life. The spectra of γ rays coincident with the 181.9- and 211.6-keV γ rays are shown in Figure 7. From the ratio of K x-rays to 68.5-keV γ rays in coincidence with the 211.6-keV γ ray, we determined α_K(68.5)=61±5. This agrees with the theoretical[31] α_K(M2)=64 and gives a B(M2)=2.5×10^{-5}. From the relative intensities of the 29.7- and 68.5-kev γ rays in the 181.9-keV gate we determined that α_{tot}(29.7)=44(15) and the 29.7-keV transition is M1+6(3)%E2. An alternative assignment of E1+4(1)%M2 is ruled out on the basis of the single-particle Weisskopf estimate of 44 μs for this transition. The total K x-ray intensity is consistent with M1, E1, or E2 assignments for the 181.9- and 211.6-keV γ rays. From the systematics of heavier odd-odd Tb we expect a negative parity isomer (see the discussion below). Assuming that the 98.3-keV transition has E3 multipolarity, consistent with a reasonable B(E3)=0.026 value, we can assign a 5$^-$ spin to the isomer, 2$^+$ to the 181.9-keV level and 3$^+$ to the 211.6-keV level. No β-decay was observed from ^{142}Tb^m. Indirect population of the 4$^+$ and 6$^+$ levels in ^{142}Gd would characterize this decay. We observe weak feeding of the the 4$^+$ level by ^{142}Tb^g decay, however the intensity of this branch remains constant in equilibrium with ^{142}Dy and is therefore not due to ^{142}Tb^m. We can set an 0.5% upper limit on the β-decay branch assuming the decay populates only levels which deexcite through the 4$^+$

level. This lack of β decay confirms our assignment of the β-delayed proton activity to ^{142}Tb^g. The isomeric decay scheme of ^{142}Tb^m is shown in Fig. 8. A second isomer in ^{142}Tb with a half-life of 15 μs which presumably de-excites to the 5$^-$ level has also been reported,[32] but was not observed in these experiments.

F. ^{142}Dy

A single 181.9-keV γ-ray transition, deexciting the level of that energy in ^{142}Tb, was assigned to ^{142}Dy decay on the basis of half-life and coincidence with Tb K x-rays and 511-keV annihilation radiation. This transition, also observed in the 303 ms ^{142}Tb^m decay (Section IV.E), decays with a longer 2.3(3) s half-life component, consistent with the half-life measured for the ^{142}Dy delayed proton branch. The total intensity of the 181.9-keV transition is 6(2)% indicating that the 2$^+$ 181.9 keV level is populated by γ transitions from higher levels in ^{142}Tb fed by allowed β transitions from the even-even ^{142}Dy. Assuming no strong γ-ray transitions were missed, the ^{142}Dy decay predominantly populates the ground state of ^{142}Tb with a logft=4.1. This confirms the 1$^+$ assignment to the ^{142}Tb ground state (see also Fig. 8).

G. ^{140}Eu^g

We have assigned 20 γ-rays to the decay of ^{140}Eu. The γ-ray energies and intensities are summarized in Table X. We have adopted a 1.51(2) s half-life for ^{140}Eu^g decay assuming two half-life components for the 531.0-keV γ ray corresponding to feeding in equilibrium with ^{140}Gd decay and direct production. This value agrees within uncertainties with 1.3(2) s from Redon et al.[10] and 1.54(13) s from Deslauriers et al.[33] The spectrum of γ rays in coincidence with Sm K x-rays is shown in Fig. 9 and the ^{140}Eu^g decay scheme is shown in Fig. 10. The firm daughter spin assignments are from ^{140}Sm in-beam reaction studies.[30] Strong β-feeding is observed to the ground(0$^+$) and first-excited(2$^+$) states of ^{140}Sm constraining the ^{140}Eu ground

state to 1^+. This assignment conflicts with the 2^+ assignment by Turcotte et al.[11], but is consistent with heavier even-even Eu isotope ground states. The decay of ^{140}Gd, discussed below, also confirms the 1^+ assignment. Weak population of the 4^+ level in ^{140}Sm has been observed and is most probably due to the deexcitation of higher-lying 2^+ levels.

H. ^{140}Eu^m

A 185.3-keV γ ray was observed to decay with a single-component half-life of 125(2) ms in the 1.6-s dwell time data. The decay curve for this transition is shown in Fig. 11. This γ ray was not found in coincidence with any transitions. Similar short half-life components were observed for the 174.8-keV γ ray deexciting the first-excited state in ^{140}Eu (see below) and for Eu K x-rays. We have thus assigned the 125(2) ms half-life to an isomer in ^{140}Eu. The intensities of the x-rays and γ rays assigned to ^{140}Eu^m decay are also given in Table X. The multipolarity of the 174.8-keV transition is M1 from Ref. 11, and, if we assume that all of the observed Eu K x-rays for ^{140}Eu^m decay are from the internal conversion of the 174.8- and 185.3-keV transitions, we derive α_K(exp)=0.19(4) for the 185.3-keV transition. This is consistent with the theoretical[31] value α_K(theory)=0.19 for an E2 transition. There is insufficient Eu K x-ray intensity for the 185.3-keV transition to have M2 or higher multipolarity so it is doubtful that the 185.3-keV level is the isomeric state. We have assigned the 174.8- and 185.3-keV levels as 2^+ and 3^+, respectively. This is consistent with significant indirect feeding of the 174.6-keV level by ^{140}Gd decay and negligible indirect feeding to the 185.3-keV level. No Eu K x-ray intensity can be associated with the isomeric transition, establishing its energy at less than the Eu K binding energy of 48.5 keV and consequently sets an upper limit of 234 keV for the isomer energy in ^{140}Eu (see Fig. 8).

From the recommended upper limits for γ-ray transition probabilities,[34] the isomeric transition must be M2 or E3. This constrains the isomer to a spin of 5^- if both lower levels are directly populated. Based on the intensity of the 185.3-keV γ-ray, we can derive B(M2) values ranging from 6×10^{-5} to 2×10^{-4},

corresponding to isomeric transition energies of 10- to 48-keV, respectively. This is consistent with the degree of hindrance observed for M2 transitions in this region. A similar estimate of B(E3) for the transition feeding the 174.6-keV level yields values substantially exceeding 1 W.U., contrary to expectations based on systematics of E3 transitions. This indicates that most of the observed intensity of the 174.6 γ-ray is due to a 10.7-keV M1 transition (which cannot be observed directly in our experiments) between the 185.3- and 174.6-keV levels.

No EC/β^+ decay was observed with ^{140}Eu^m decay. This decay mode would presumably populate the 4$^+$ level in ^{140}Sm, yet no short-lived component was observed for the 715.4-keV level depopulating that state. From the relative intensity of the 174.8-, 185.3-, and 715.4-keV transitions, we can set an upper limit of 1% on the EC/β^+ branching intensity.

I. ^{140}Gd

We have assigned 32 γ-rays to the decay of ^{140}Gd. The γ-ray energies and intensities are summarized in Table XI where they are compared with those of Turcotte et al.[11] Our energies agree with Ref. 11, however there is again poor agreement with the intensities, especially with regard to the intense 750 keV transition. It is not apparent why the agreement is so poor except for the fact the no chemical or mass separation was performed in Ref. 11. From the decay of the strongest γ rays, we determined a 15.8(4) s half-life for ^{140}Gd. This agrees with 16.2(8) s from Turcotte et al.[11] but not with 11(2) s by Redon et al.[10] Habs et al.[6] reported a 20 s isomer of ^{140}Eu based on the observed decay of a 531-keV γ ray with that half-life. It is now apparent that they produced that transition from the decay of ^{140}Eu^g in equilibrium with ^{140}Gd.

The spectrum of γ rays in coincidence with Eu K x-rays is shown in Fig. 12, and the decay scheme for ^{140}Gd decay is shown in Fig. 13. The ^{140}Eu level scheme below 750 keV is similar to that of Turcotte et al.[11] Significant discrepancies exist only for higher levels. We observe substantial β-decay to the ^{140}Eu ground state which is consistent with our 1$^+$ assignment and not the 2$^+$ assigned in Ref. 11. The 174.6- and

191.2-keV levels are not significantly populated by β-decay; this is inconsistent with their previous 1$^+$

assignments.[11] Higher levels are too weakly populated to confirm 1$^+$ assignments with the exception of the

749.9-keV level where the logft=4.4 is indicative of a definite 1$^+$ spin and parity.

J. ^{140}Tb

Two γ-rays with energies of 328.4- and 627.8-keV have been assigned to ^{140}Tb decay on the basis of coin-

cidence with Gd K x-rays. The relevant γ spectrum is shown in Fig.14. The 328.4-keV γ ray decays with a

single-component 2.4(2) s half-life. Both γ-rays were observed in in-beam reaction studies of ^{140}Gd[35] and

assigned to the 2$^+$→0$^+$ and 6$^+$→4$^+$ transitions. The intensities of these γ-rays are given in Table X. The

4$^+$→2$^+$ transition is known[35] to be 508-keV and could not be resolved from the intense 511-keV annihila-

tion radiation. The 627.8-keV transition is about one-half of the intensity of the 328.4-keV transition

which is consistent with significant β-feeding and a spin of 5,6, or 7 for the ^{140}Tb parent. No evidence for

the 675-keV 8$^+$→6$^+$ transition was observed. Fig. 15 shows the decay scheme for ^{140}Tb. Here we have

assumed that nearly all of the decay populates levels which deexcite through the 4$^+$ or 6$^+$ levels in ^{140}Gd.

From the relative intensities of the 328.4- and 627.8-keV γ -rays we conclude that about half of the beta

decay directly or indirectly populates each of these two levels. Very little Gd K x-ray intensity is observed

with this decay so feeding to high-lying levels must be minimal. Based on these assumptions, we derive

Q_{EC}>11.3 MeV, in agreement with the value of 10.7(11) MeV from Wapstra et $al.$[12] From the apparent low

logft or intense γ-ray feeding to the 4$^+$ and 6$^+$ levels, we conclude the ^{140}Tb spin is probably 5. We cannot

determine whether the 2.4-s higher-spin Tb is the ground state or an isomer. However, no Tb K x-rays

were observed indicating that there is no isomeric transition from this state (or that the IT energy is less

than 50 keV). From the systematics of the heavier odd-odd Tb isotopes,[38] one should expect a 1$^+$ ground

state with a half-life considerably shorter than 1 s. This state would be only weakly populated in this reac-

tion and decay mostly to the ^{140}Gd ground state; thus it would probably have escaped detection in these

experiments.

V. CONCLUSIONS

The Q_{EC} values deduced from the radioactive decay schemes described in this paper are in good agreement with both the evaluated values of Wapstra and Audi,[12] and the calculated values of Liran and Zeldes.[13] This agreement suggests that statistical feeding to high-lying daughter levels in the A=142 and A=140 mass chains is low or even negligible. The principal reason for this result is the preponderance of $1^+ \rightarrow 0^+$ and $0^+ \rightarrow 1^+$ ground-state to ground-state β-transitions with low logft values in these even mass decay chains. The β strength is strongly dominated by these fast transitions and leaves little remaining intensity to be apportioned statistically at higher excitation energies. This point is emphasized when we compare (Table IV) the measured half-lives with those calculated from the gross β decay theory.[36,37] Agreement for the even-even parents is typically within a factor of 2-3 while odd-odd decays are calculated to be about an order of magnitude longer-lived than is observed. Inspection of the gross theory beta strength model reveals that it underestimates the strength of decay to levels below the pairing gap in the even-even daughter nuclei. The odd-odd parent beta strength to the even-even daughter ground-state is therefore neglected, while even-even parent decays are assumed to have considerable beta strength to levels near the daughter's ground state. If we were to include the measured ground state beta strength in the calculation the agreement between the gross theory and the experimental values would become much better. This same effect can also explain the discrepancy noted in Section III.D between the experimental β-delayed proton decay branch for the odd-odd low spin precursor $^{142}Tb^g$ and the value calculated with a QRPA model.[25,26] However, good agreement was obtained for both the even-even precursor ^{142}Dy and the odd-odd, $J^\pi=5$ precursor ^{140}Tb (see Table VI). Like the gross theory, the QRPA beta strength model tends to underestimate the strength of ground state β transitions from low spin odd-odd nuclei and therefore overestimates calculated half-lives and delayed proton branches.

The logft values for the $0^+ \rightarrow 1^+$ and $1^+ \rightarrow 0^+$ ground-state beta transitions are all less than 5. Below N=82

and above Z=58, the $\pi d_{5/2} \rightarrow \nu d_{3/2}$ spin-flip transition is expected to be fast, and above Z=64 the

$\pi h_{11/2} \rightarrow \nu h_{9/2}$ transition is important. In the even-even nuclei either a $(\pi d_{5/2})^2$ or a $(\pi h_{11/2})^2$ pair are

assumed to decay, and in odd-odd parents the odd proton and neutron are expected to recouple. The sys-

tematics[38] of the logft values for the even-even transitions are plotted in Fig. 16(a). The shell model

predicts,[39]

$$ft = \frac{6160}{g_a^2 B(GT)} \qquad (2)$$

where $g_a = 1.263$, $B(GT) = n\frac{4l}{2l+1}$, and n is the number of valence protons. These predictions are shown in

fig. 16(b) and are nearly an order of magnitude lower than experiment. This phenomenon has been com-

mented on previously by Nolte et al.[40] for the N=82 region and by Barden et al.[41] for the Z=50 region

($\pi g_{9/2} \rightarrow \nu g_{7/2}$ transitions). Towner[42] has argued that these discrepancies are due to pairing correlations,

core polarization, and higher-order phenomena.

The n dependence predicted by the shell model (Eq. 2) appears to persist in the spin-flip transitions where

the average logft value changes between $n=2$ and $n=6$ by 0.54(12) for N=76-78, Z=60-64, and by 0.40(6)

for N=82-86, Z=66-70. These values agree with the expected value of 0.48 from Eq. 2. The N=80 transi-

tions were excluded from the first average because the shell model predicts that the $\nu d_{3/2}$ orbital is filled,

blocking the spin-flip transition. This is demonstrated by comparing the N=76 and N=78 logft values.

They differ by 0.22(12), consistent with an 0.3 predicted difference if the $\nu d_{3/2}$ orbital were half-filled at

N=78. Experimentally, a nearly constant logft=5.0 is observed for all decays with N=80. The $\nu s_{1/2}$ and

$\nu d_{3/2}$ orbital are nearly degenerate in this region, perhaps explaining the residual β-strength at N=80.

The systematics[38] of the $1^+ \rightarrow 0^+$ decays are shown in Fig. 17. As in the neighboring $0^+ \rightarrow 1^+$ transitions, the

logft values for N=79 and Z=59-63 decrease by 0.50(11) from $n=1$ to $n=5$, which is slightly less than the

0.70 value predicted by the shell model. This trend is not observed for N=81 where the spin-flip transition

is blocked. It is remarkable that these shell model trends are sustained despite the fact that the logft values

are hindered. However, the calculations by Towner[42] suggest that the hindrance should be constant for the

l=5 orbitals. Similar shell model trends have also been reported for isomeric E2 transitions in N=82 nuclei.[40,43-46]

Another interesting feature is the low $\log ft$ values for ^{142,144}Dy. The valence protons in these isotopes should be $(\pi h_{11/2})^2$ yet the $\nu h_{9/2}$ neutron orbital lies above the N=82 shell gap. We thus expect the ground-state transition to be dominated by the $\pi d_{5/2} \rightarrow \nu d_{3/2}$ transition. The $\pi d_{5/2}$ orbital is filled at Z=64 so we expect the $\log ft$ values in the light Dy isotopes to be similar to the adjacent Gd decays. The $\log ft$ values reported here are much lower than expected and seem consistent with the Dy decay for N>82. It is likely that the ^{142,144}Dy log values are low due to missed β-strength to levels near 2 MeV from the $\pi h_{11/2} \rightarrow \nu h_{9/2}$ transition. This transition was observed in ^{146}Dy decay[47] with a $\log ft$=3.8(2) that is consistent with the heavier Dy decays. Assuming that this transition occurs with the same $\log ft$ in the lighter Dy isotopes, about 35% of the decay would populate that resonance in ^{142}Tb raising the $\log ft$ for the ground state transition to a value comparable to ^{140}Gd decay. For ^{144}Dy decay the $\pi h_{11/2} \rightarrow \nu h_{9/2}$ branch would be only ~7% which is, however, insufficient to raise the ground-state $\log ft$ to the ^{142}Gd value.

As can be seen from Fig. 8, the ^{140}Eu^m and ^{142}Tb^m decays are remarkably similar. The similarity of these decays, despite their straddling the semi-magic Z=64 shell may be indicative of a common structure and of the disappearance of that shell below N=78.[14,48] From the well characterized systematics of the N=77 isotones it has been established that the odd neutron should be in either a 1/2$^+$ or an isomeric 11/2$^-$ orbital, presumably related to the $\nu s_{1/2}$ and $\nu h_{11/2}$ shell model states. In our investigation of ^{141}Tb decay,[14] we assigned J$^\pi$=5/2$^-$ to the ground-state and suggested a 5/2[532] configuration. ^{143}Tb has been assigned J$^\pi$=5/2^{+} [10] and may be the 5/2[402] configuration, although other neighboring configurations are possible. The 5/2[402] configuration cannot be coupled with the expected neutron configuration to explain the 5$^-$ for both odd-odd N=77 isomers. However, the expected shell model state at at Z=65 is $\pi s_{1/2}$, which can be coupled with the $\nu h_{11/2}$ neutron to explain the measured spin. At Z=63, the $\pi d_{5/2}$ shell model state is expected which also cannot couple with the odd neutron to give 5$^-$. Alternate proton configurations for

Z=63 and/or Z=65 include 1/2[550] and 1/2[411], both of which lie near the proposed configurations for ^{141,143}Tb and could give rise to the correct spin.

For ^{142}Tb^m decay we determine that the single particle B(M2)~2.5×10^{-5} and B(E3)~0.026 transition probabilities are very hindered. This is likely if the neutron Nilsson configurations for the 2$^+$ and 3$^+$ all have low K quantum numbers. The M2 transition in ^{140}Eu^m is also very hindered, but the B(M2)~(2 to 6)×10^{-4} is almost an order of magnitude larger than that for the corresponding transition in ^{142}Tb.

The A=140 and A=142 isotopes in this study are close to the Z=64 shell closure which is predicted to disappear near N=78. The A=140 isotopes cross Z=64 at N=76 and are expected to show signs of significant deformation.[14,48] Since our experiments sample predominantly 0$^+$ and 1$^+$ states, no conclusive and unambiguous evidence for such deformation or for the disappearance of the shell gap near ^{142}Gd could be found in the data.

ACKNOWLEDGEMENTS

REFERENCES

1. J. Gilat, J.M. Nitschke, P.A. Wilmarth, and R.B. Firestone, Bulletin American Physical Society 31,1212 (1986).

2. J. Gilat, J.M. Nitschke, P.A. Wilmarth, K. Vierinen, and R.B. Firestone, *Proceedings 5th International Conference on Nuclei Far From Stability, Rousseau Lake, Ontario, 1987*, edited by I.S. Towner (AIP Conference Proceedings, New York, 1988) p. 463.

3. L.K. Peker, Nucl. Data Sheets **43**, 579 (1984).

4. D. Habs, H. Klewe-Nebenius, R. Lohken, S. Goring, J. van Klinken, H. Rebel, and G. Schatz, Z. Phys. **A250**, 179 (1972).

5. G.G. Kennedy, S.C. Gujrathi, and S.K. Mark, Phys. Rev. **C12**, 553 (1975).

6. D. Habs, et al., KFK-1783, p. 47 (1973).

7. R. Turcotte, H. Dautet, and S.K. Mark, Z. Phys. **A330**, 349 (1988).

8. L. Westgaard, the ISOLDE Collaboration, Bull. Amer. Phys. Soc. **17**, 907, CB13 (1972).

9. R. Beraud, R. Duffait, A. Emsallem, M. Meyer, N. Redon, D. Rolando-Eugio, D. Barneoud, J. Blachot, J. Genevey, A. Gizon, *Proceedings Third International Conference on Nucleus Nucleus Collisions, Saint-Malo, France, 1988*, edited by C. Esteve, C. Gregoire, D. Guerreau, and B. Tamain (Centre de Publications de L'Universite de Caen, 14032 Caen Cedex, France, 1988) p. 3.

10. N. Redon, T. Ollivier, R. Beraud, A. Charvet, R. Duffait, A. Emsallem, J. Honkanen, M. Meyer, J. Genevey, A. Gizon, and N. Idrissi, Z. Phys **A325**, 127 (1986).

11. R. Turcotte, H. Dautet, S.K. Mark, E. Hagberg, V.T. Koslowsky, J.C. Hardy, and H. Schmeing, Z. Phys. **A331**, 109 (1988).

12. A.H. Wapstra and G. Audi, Nucl. Phys. **A432**, 140 (1985).

13. S. Liran and N. Zeldes, At. Data Nucl. Data Tables **17**, 431 (1976).

14. J. Gilat, J.M. Nitschke, P.A. Wilmarth, and R.B. Firestone, Phys. Rev. **C40**, 2249 (1989).

15. J.M. Nitschke, Nucl. Instrum. Meth. **206**, 341 (1983).

16. J.T. Routti and S.G. Prussin, Nucl. Instrum. Meth. **72**, 125 (1969).

17. R.A. Belshe and M.K. Lee, Nucl. Instrum. Phys. Res. **A253**, 65 (1986).

18. R.A. Belshe, SUSIE Reference Manual, Lawrence Berkeley Laboratory, PUB-3061 (1987).

19. R.A. Belshe, EVA Reference Manual, Lawrence Berkeley Laboratory, PUB-3062 (1987).

20. *Table of Isotopes* (1978), 7th Edition, Editors: C.M. Lederer and V.S. Shirley, Authors: E. Browne, J.M. Dairiki, R.E. Doebler, A.A. Shihab-Eldin, L.J. Jardine, J.K. Tuli, and A.B. Buryn, John Wiley, New York.

21. E. Bambynek, B. Crasemann, R.W. Fink, H. -U. Freund, H. Mark, C.D. Swift, R.E. Price, and P.V. Rao, Rev. Mod. Phys. **44**, 716 (1972).

22. N.B. Gove and M.J. Martin, At. Data Nucl. Data Tables **A10**, 205 (1971).

23. G. Azuelos and J.E. Kitching, At. Data Nucl. Data Tables **17**, 103 (1976).

24. RLMUL, International Mathematical and Statistical Library (IMSL) code for multilinear analysis of data.

25. P.A. Wilmarth, Ph.D. Thesis, University of California, Berkeley, 1988, Lawrence Berkeley Laboratory Report LBL-26101.

26. J. Krumlinde and P. Moller, Nucl. Phys. **A417**, 419 (1984)

27. M.K. Dewanjee, and I.L. Preiss, J. Inorg. Nucl. Chem. **34**, 1105 (1972).

28. G.L. Struble, L.G. Mann, R.G. Lanier, W.M. Buckley, J. Kern, G. Crawley, S. Gales, D. Muller, and F. Girshick, Phys. Rev. **C23**, 2447 (1981).

29. S.Lunardi, F. Soramel, W. Starzecki, W. Meczynski, R. Julin, M. Lach, A. Ercan, and P. Kleinheinz, Z. Phys. **A324**, 433 (1986).

30. W. Starzecki, G. de Angelis, B. Rubio, J. Styczen, K. Zuber, H. Guven, W. Urban, W. Gast, P. Kleinheinz, S. Lunardi, F. Soramel, A. Facco, C. Signorini, M. Morando, W. Meczynski, A.M. Stefanini, and G. Fortuna, Phys. Lett. **200**, 419 (1988).

31. F. Rosel, H.M. Fries, K. Alder, and H.C. Pauli, At. Data Nucl. Data Tables **21**, 291 (1978).

32. I. Zychor, S. Hofmann, F.P. Hessberger, and G. Munzenberg, GSI Annual Report 1988, GSI-89-1 (1989).

33. J. Deslauriers, S.C. Gujrathi, and S.K. Mark, private communication, (1986); referenced in L. Peker, Nucl. Data Sheets **51**, 395 (1987).

34. P.M. Endt, At. Data Nucl. Data Tables **26**, 47 (1981).

35. C.J. Lister, B.J. Varley, R. Moscrop, W. Gelletly, P.J. Nolan, D.J.G. Love, P.J. Bishop, A. Kirwan, D.J. Thornley, L. Ying, R. Wadsworth, J.M. O'Donnell, H.G. Price, and A.H. Nelson, Phys. Rev. Lett. **55**, 810 (1985).

36. K. Takahashi, M. Yamada, and T. Kondoh, At. Data Nucl. Data Tables **12**, 101 (1973).

37. K. Takahashi, private communication (1988).

38. R.B. Firestone, J.M. Nitschke, P.A. Wilmarth, K.S. Vierinen, R.M. Chasteler, J. Gilat, and A.A. Shihab-Eldin, *Proceedings of the Symposium on Exotic Nuclear Spectroscopy, Division of Nuclear Chemistry and Technology, American Chemical Society, Miami Beach, FL, 1989*, in press; and Lawrence Berkeley Laboratory Report LBL-28172.

39. R.D. Lawson, *Theory of the Nuclear Shell Model* (Clarendon, Oxford, 1980).

40. E. Nolte, G. Korschinek, and Ch. Setzensack, Z. Phys. **A309**, 33 (1982).

41. R. Barden, R. Kirchner, O. Klepper, A. Plochocki, G.-E. Rathke, E. Roeckl, K. Rykaczewski, D. Schardt, and J. Zylicz, Z. Phys. **A329**, 319 (1988).

42. I.S. Towner, Nucl. Phys. **A444**, 402 (1985).

43. P.J. Daly, P. Kleinheinz, R. Broda. A.M. Stefanini, S. Lunardi, H. Backe, L. Richter, R. Willwater, and F. Weik, Z. Phys. **A288**, 103 (1978).

44. H. Helppi, Y.H. Chung, P.J. Daly, S.R. Faber, A. Pakkanen, I. Ahmad, P. Chowdhury, Z.W. Grabowski, T.L. Khoo, R.D. Lawson, and J. Blomqvist, Phys. Lett. **115B**, 11 (1982).

45. E. Nolte, G. Colombo, S.Z. Gui, G. Korschinek, W. Schollmeier, P. Kubik, S. Gustavsson, R. Geier, and H. Morinaga, Z. Phys. **A306**, 211 (1982).

46. J. H. McNeil, J. Blomqvist, A.A. Chishti, P.J. Daly, W. Gelletly, M.A.C. Hotchkis, M. Piiparinen, B.J. Varley, and P.J. Woods, Phys. Rev. Let. **63**, 860 (1989).

47. K. Zuber, C.F. Liang, P.Paris, J. Styczen, J. Zuber, P. Kleinheinz, B. Rubio, G. de Angelis, H. Gabelmann, A. Huck, J. Blomqvist, and the ISOLDE collaboration, CERN, Z. Phys. **A327**, 357 (1987).

48. J.A. Cizewski and E. Gulmez, Phys. Lett. **B175**, 11 (1986).

Table I. A=142 Coincidence Results

Gate	Coincidences
Sm K x-rays	683,768,864,890,1287,1405, 1658,1671,1754,2056,2264, 2354,2374,2420
683	768
768	683,890,1287,1405,1671, 1754,2264,2420
890	768
1287	768
1405	768
1754	768
2264	768
Eu K x-rays	179,212,223,242,280,284, 307,348,407,503,526,551, 586,591,614,620,632,651, 661,705,732,750,821,824, 853,862,911,936,1000,1133, 1154,1187,1204,1234,1260, 1275,1412,1438,1495,1600, 1779,1847,1949,1957,1982
179	101,223,348,(375),407,482, 572,821,1204,1234,1260, (1275),1302,1307,1600, 1847,1982
212	136,(239),284
216	280
280	223,(228),264,335,472, 910,1133,(1275)
284	212,242,307,330,336,448, 651,1154,1496
526	105
615	824
620	1158
Gd K x-rays	(389),465,515,693,853, (934),980
465	(389),465,515
515	(389),465,693,853,1399,1587, 1799
853	515
980	389,465
1399	515
Tb K x-rays	30,69,182,212
182	30,69,99
212	69

Table II. A=140 Coincidence Results

Gate	Coincidences
Sm K x-rays	460,531,609,715,1068, 1098,1294,1402,1420, 1491,1753,1952
460	531,609
531	460,1068,1098,1402,1491, 1753,(1759)
609	460,531
685	531
715	531
1068	531
1098	531
1491	531
1753	531
2065	531
Eu K x-rays	175,185,191,237,262,272, 278,297,304,314,344,379, 418,428,436,447,453,496, 546,575,708,722,750,902, 918,1041,1131
175	185,272,278,297,314,372, 436,575,708,902,918,1041
191	237,262,344,496,558
262	191,269
272	175
297	175
453	269
750	292
Gd K x-rays	328,628

Table III. Comparison of experimental and theoretical K x-ray intensities for A=142 isotopes

	K_{α_1}		K_{α_2}		K_{β_1}'		K_{β_2}'	
	Expt	Th	Expt	Th	Expt	Th	Expt	Th
Nd	100(2)	100	50(4)	54.9	24(8)	30.0		8.3
Pm	100.0(12)	100	53.6(8)	55.1	30.6(12)	30.1		8.4
Sm	100.0(13)	100	54.6(7)	55.2	31.0(3)	30.2	8.8(3)	8.6
Eu	100.0(10)	100	55.7(8)	55.4	30.9(6)	30.5	8.5(2)	8.7
Gd	100(8)	100	43(9)	55.6		30.8		8.9
Tb	100(3)	100	50(2)	55.8	34(4)	31.0	10(3)	8.9

Table IV. Summary of experimental and theoretical half-lives and decay branching intensities for A=142 and A=140

Isotope	$t_{1/2}$		Branching intensity		E_γ	I_γ^c	I_γ^d
	Experiment[a]	Theory[b]	β^+	EC			
^{142}Pm	40.5(5) s	540 s	0.771(27)	0.229(27)	1576.1	0.0196(11)	
^{142}Sm	72.49(5) min	22 m	<0.05	>0.95			
^{142}Eu	2.34(12) s	54 s	0.899(16)	0.101(16)	768.0	0.102(7)	≡0.102(3)
^{142}Gd	70.2(6) s	80 s	0.48(5)	0.52(5)	178.9	0.112(12)	0.113(5)
^{142}Tb	597(17) ms	3.5 s	0.968(4)	0.032(4)	515.3	0.249(17)	≡0.249(13)
^{142}Dy	2.3(3) s	4.3 s	0.90(4)	0.10(4)	181.3	0.043(8)	0.051(5)
^{140}Eu[g]	1.51(2) s	15 s	0.951(7)	0.049(7)	531.0	0.29(5)	0.30(3)
^{140}Gd	15.8(4) s	41 s	0.67(8)	0.33(8)	749.9	0.110(15)	≡0.110
^{140}Tb	2.4(2) s	1.5 s	>0.97	<0.03	328.4	0.96	

[a] Values for ^{142}Pm and ^{142}Sm are from L.K. Peker, Nucl. Data Sheets **43**, 579 (1984). Other values from this work.

[b] From Gross Theory, K. Takahashi, M. Yamada, and T. Kondoh, At. Data and Nucl. Data Tables **12**, 101 (1973) and private communication (1988).

[c] Normalized to measured EC+β^+ intensity.

[d] Equilibrium intensity normalized to the indicated equilibrium partner.

Table V. Comparison of experimental and theoretical Q_{EC} values

Isotope	Q_{EC}(MeV)		
	Experiment	Wapstra and Audi[a]	Liran and Zeldes[b]
^{142}Dy	7.1(2)		7.1
^{142}Tb[g]	10.4(7)		9.9
^{142}Gd	4.2(3)	4.4(4)	4.6
^{142}Eu[g]	7.0(3)	7.40(10)	7.5
^{142}Sm	<2.1	2.09(5)	2.2
^{142}Pm	4.88(16)	4.89(5)	5.1
^{140}Tb	>11.3	10.7(11)	10.9
^{140}Gd	4.8(4)	4.5(7)	5.5
^{140}Eu[g]	8.4(4)	8.4(4)	8.3

[a]A.H. Wapstra and G. Audi, Nucl. Phys. **A432**, 140 (1985).

[b]S. Liran and N. Zeldes, At. Data Nucl. Data Tables **17**, 431 (1976).

Table VI. Comparison of experimental and calculated half-lives and delayed proton branching ratios.

Isotope	$t_{1/2}$(exp)	$t_{1/2}$(QRPA)[a]	$t_{1/2}$(GT)[b]	P_p(exp)	P_p(QRPA)[a]	P_p(GT)[b]
^{142}Dy	2.3(3) s	2.7 s	4.2 s	$6(3)\times10^{-4}$	1×10^{-3}	1×10^{-3}
^{142}Tb^g	597(17)ms	3.5 s	4.9 s	$2.2(11)\times10^{-5}$	3×10^{-4}	3×10^{-4}
^{140}Tb	2.4(2) s	2.0 s	2.2 s	$2.6(13)\times10^{-3}$	3×10^{-3}	1×10^{-3}

[a]Calculated using QRPA model; J. Krumlinde and P. Moller, Nucl. Phys. **A417**, 419 (1984); P.A. Wilmarth, Ph.D. Thesis, University of California, Berkeley, 1988, LBL Report 26101.

[b]Calculated using the gross theory of beta decay, K. Takahashi, M. Yamada, and T. Kondoh, At. Data. Nucl. Data Tables **12**, 101 (1973) and private communication (1988).

Table VII. Transition energies, level assignments, and relative intensities for ^{142}Eu^g decay

E_γ(keV)	Level Energy	I_γ(rel) This work[a]	I_γ(rel) Kennedy et al.[b]
683.0(1)	1451.1	4.1(4)	5.5(8)
768.1(1)	768.1	100	100
864.4(2)	2522.2	0.84(18)	
889.8(1)	1657.9	10.4(7)	13.3(12)
1287.4(1)	2055.6	11.4(8)	13.7(12)
1405.4(1)	2173.6	4.0(4)	7.1(8)
1451.1[c]	1451.1	~2	
1657.9(1)	1657.9	17.2(13)	13.0(30)
1754.1(1)	2522.2	14.6(12)	13.0(10)
2055.8(2)	2055.6	4.4(4)	4.9(6)
2263.7(4)	3031.9	4.9(11)	
2353.7(3)	2353.7	5.2(10)	
2373.9(3)	2373.9	7.5(9)	
2419.7(2)	3187.9	2.4(9)	

[a]For absolute intensity per 100 decays of ^{142}Gd, multiply by 0.102(7)

[b]G.G. Kennedy, S.C. Gujrathi, and S.K. Mark, Phys. Rev. C12, 553 (1975).

[c]E0 transition intensity inferred from excess Sm K x-ray coincidence intensity.

Table VIII. Transition energies, level assignments, and relative intensities for ^{142}Gd decay

E$_\gamma$(keV)	Level Energy	I_γ(rel) This work[a]	I_γ(rel) Turcotte et al[b]	E$_\gamma$(keV)	Level Energy	I_γ(rel) This work[a]	I_γ(rel) Turcotte et al[b]
101.4(1)	280.2	0.92(23)	0.88(15)	631.7(1)	631.7	9.5(8)	
105(1)[c]	631.7	~1		651.3(1)	935.6	2.9(4)	2.0(9)
136(1)[c]	631.7	~1		660.9(1)	660.9	4.3(5)	
178.9(1)	178.9	100.0(15)	100	704.9(1)	704.9	7.9(22)	7.1(15)[d]
203(1)[c]	935.6	~0.8	0.85(17)[d]	732.4(1)	732.5	5.1(4)	
212.2(1)	496.6	1.53(15)		750.2(1)	750.2	7.2(7)	
216(1)[c]	496.6	~0.5		821(1)[c]	1000.2	~2	
222.8(1)	503.0	14.4(6)	20.5(6)[d]	823.9(1)	1438.4	10.8(25)	
228(1)[c]	732.5	~0.9	2.1(18)[d]	853(1)[c]	1438.4	~1.1	1.3(3)[d]
238.8(1)		1.3(2)		862(1)[c]	1412.9	~3	0.5(4)[d]
241.7(2)	526.2	1.5(4)	4.5(3)	886.3(2)			2.9(13)[d]
247.2(1)	750.2	1.60(23)	2.6(6)	910.0(1)	1412.9	2.4(5)	4.2(11)[d]
264.2(1)	544.4	4.1(3)		912.0(2)			2.9(6)[d]
274.3(4)			b	935.6(1)	935.6	4.4(5)	9.6(21)[d]
280.3(1)	280.2	35.9(8)	38.4(4)	1000.2(1)	1000.2	14(2)	
284.4(1)	284.4	55.0(15)	53.9(5)	1073.6(4)			b
306.9(1)	591.3	7.2(5)	2.6(8)[d]	1133(1)[c]	1412.9	~1.3	1.8(4)
330.4(1)	614.6	2.9(5)	6.5(28)[d]	1153.8(1)	1438.4	2.1(5)	5.5(5)
335(1)[c]	614.6	~2	1.5(12)[d]	1158(1)[c]	1779.1	~2	
336(1)[c]	619.7	~0.5		1187(1)[c]	1779.1	~6	1.7(8)[d]
347.6(1)	526.2	4.0(6)	2.6(5)[d]	1204.4(1)	1383.3	4(2)	
375.4(1)		2.5(3)		1233.9(1)	1412.9	15.0(8)	14.6(29)[d]
407.0(1)	585.7	4.8(4)	5.7(4)	1259.6(1)	1438.4	38.2(15)	29.9(6)[d]
448.2(1)	732.5	1.8(4)	2.6(5)[d]	1275(1)[c]	1779.1	~2	7.0(7)[d]
466(1)[c]	750.2		b	1302(1)[c]	1480.9	~3	
472(1)[c]	750.2	~1	b	1307(1)[c]	1485.9	~1	
503.0(1)	503.0	6.4(15)	b	1412.4(2)	1412.9	6.8(15)	
526.2(1)	526.2	52.7(15)	38.9(15)	1438.4(2)	1438.4	11(4)	
550.6(1)	550.6	6.4(7)	5.6(12)	1495.0(2)	1779.1	5.9(15)	4.9(6)
553(1)[c]	732.5	~5		1599.7(2)	1779.1	18(3)	8.3(7)[d]
572(1)[c]	750.2	~5	3.5(20)[d]	1779.1(1)	1779.1	22.1(23)	
585.7(2)	585.7	4.7(6)		1846.7(2)	2025.6	6(3)	
591.3(1)	591.3	9.8(7)		1948.6(3)	1948.6	9(4)	
595.9(3)			2.1(15)[d]	1956.6(3)	1956.6	7(3)	
614.5(1)	614.6	13.0(8)	10.8(4)	1982(1)[c]	2160.9	~2	2.8(14)[d]
619.7(1)	619.7	18.3(8)	13.3(5)				

[a]For absolute intensity per 100 decays of ^{142}Gd, multiply by 0.112(11)

[b]R. Turcotte, H. Dautet, and S.K. Mark, Z. Phys A330, 349 (1988).

[c]Observed only in coincidence.

[d]Intensity was obtained after subtraction of known contaminants.

Table IX. Transition energies, level assignments, and relative intensities for ^{142}Tb^g decay

E$_\gamma$(keV)	Level Energy	I$_\gamma$(rel)[a]
388.8(1)	1368.7	0.90(9)
465.0(1)[b]	980.0	11(2)
	1445.1	2(1)
515.3(1)	515.4	100(7)
693.7(1)	1209.1	4.0(5)
853.1(1)	1368.7	9.7(8)
898.4(3)	2343.9	1.1(3)
934(1)[c]	1914.7	
980.1(1)	980.0	1.8(4)
1299.6(2)	2279.6	1.6(2)
1364.1(4)	2343.9	0.8(2)
1399.2(1)	1914.7	9.6(8)
1587.4(3)	2102.8	1.4(4)
1764.1(2)	2279.6	0.9(2)
1799(1)[c]	2314	~2
1828.7(2)	2343.9	2.7(3)
1915.0(2)	1914.7	2.3(3)
2343.6(3)	2343.9	1.0(2)

[a]For absolute intensity per 100 decays of ^{142}Gd, multiply by 0.249(7)

[b]Unresolved transition, intensity divided using coincidence data. The total 465-keV transition intensity is 13.3(12).

[c]Transition observed only in coincidence.

Table X. Transition energies, level assignments, and relative intensities for $^{140}\text{Eu}^{g+m}$ and ^{140}Tb decay

Parent	E_γ(keV)	Level Energy	I_γ(rel)
$^{140}\text{Eu}^{g}$ [a]	39.5	Sm $K_{\alpha2}$	4.23(16)
	40.1	Sm $K_{\alpha1}$	7.45(30)
	45.4	Sm $K_{\beta1'}$	1.9(4)
	46.6	Sm $K_{\beta2'}$	0.63(3)
	352.4(2)[b]	1599.1	0.4(2)
	459.9(1)	990.7	11.0(8)
	531.0(1)	531.0	100(9)
	608.6(1)	1599.1	1.9(2)
	685.1(2)	2284.1	0.9(3)
	715.4(2)	1246.5	0.6(1)
	882.7(3)	2482.4	0.2(1)
	1068.0(1)	1599.1	11.0(11)
	1097.7(2)	1628.6	2.0(3)
	1293.6(1)	2284.1	1.2(2)
	1299.4(2)	2102.8	0.3(1)
	1402.2(2)	1933.2	0.9(2)
	1420.3(2)	1420.3	1.2(2)
	1491.3(2)	2482.4	2.1(3)
	1752.8(2)	2284.1	1.9(3)
	1758.7(4)	2289.9	0.4(2)
	1952.0(2)	2482.4	1.4(2)
	2064.9(3)	2595.8	3.2(6)
	2283.9(3[b])	2284.1	0.5(2)
	2289.1(5)	2289.9	0.2(1)
$^{140}\text{Eu}^{m}$ [c]		Eu $K_{\alpha,\beta}$	50(5)
	174.8(1)	174.6	100(4)
	185.3(1)	185.3	92(4)
^{140}Tb [d]		Gd $K_{\alpha,\beta}$	<6.7
	328.4(2)	328.4	100(18)
	(508)[e]	837	~100
	627.8(2)	1456	52(9)

[a]For absolute intensity per 100 decays multiply by 0.29(5)
[b]Placed in the decay scheme by energy sums
[c]For absolute intensity per 100 decays multiply by 0.39(2)
[d]For absolute intensity per 100 decays multiply by 0.96
[e]Not measured in this experiment. From C.J. Lister et al., Phys. Rev. Lett. 55, 810 (1985).

Table XI. Transition energies, level assignments, and relative intensities for ^{140}Gd decay

E_γ(keV)	Level Energy	I_γ(rel) This work[a]	I_γ(rel) Turcotte et al[b]
40.9	Eu $K_{\alpha 2}$	21.9(10)	
41.5	Eu $K_{\alpha 1}$	38.6(16)	
47.0	Eu $K_{\beta 1'}$	11.5(6)	
48.3	Eu $K_{\beta 2'}$	2.9(2)	
174.8(2)	174.6	108(19)	100
186.7(3)	361.3	3.8(13)	5.9(11)
191.2(1)	191.2	49(9)	44.8(34)
236.7(1)	427.9	8.9(13)	13.8(7)
253.3(2)	427.9	8.9(19)	
261.8(2)	453.3	7.6(13)	10.3(16)
269.0(2)	722.3	1.9(6)	
272.4(1)	447.0	0.9	10.8(13)
278.4(5)	453.3	10.1(13)	4.6(7)
296.6(2)	749.9	12.7(13)	16.2(10)
304.5(2)	722.3	1.3(6)	
313.5(3)	488.1	12.0(25)	
344.5(4)	535.7	1.9(13)	
372.0(2)	546.6	3.8(13)	
379.0(1)	284.4	54(8)	5(3)
417.7(1)	417.7	39(4)	c
427.9(2)	427.9	11.4(13)	
436.4(2)	611.0	7.0(13)	9.8(19)
446.9(3)	447.0	6.3(19)	
453.4(2)	453.3	19(6)	c
495.8(2)	687.0	9.5(13)	c
532.0(4)			9(5)
546.5(2)	546.6	20.3(19)	
558.7(3)	749.9	33(3)	
575.4(1)	749.9	39(4)	26.0(43)
686.2(4)			6(4)
708.1(2)	882.7	9.5(13)	c
722.3(1)	722.3	27(4)	46(6)
749.9(1)	749.9	100(6)	38(12)
774.6(3)			c
903.2(3)	1077.8	3.2(13)	
918(1)	1092.6	9(4)c	
982.9(4)			c
1041.4(2)	1216.0	13(6)	
1131.1(3)	1131.1	5.1(13)	5.3(23)

[a]For absolute intensity per 100 decays of ^{140}Gd, multiply by 0.70(8)
[b]R. Turcotte, H. Dautet, S.K. Mark, E. Hagberg, V.T. Koslowsky, J.C. Hardy, and H. Schmeing, Z. Phys A330, 349 (1988).
[c]Observed only in coincidence.

FIGURE CAPTIONS

FIG 1. Arrangement of detectors surrounding the mass-separated products collected with the fast-cycling tape system at OASIS.

FIG 2. Decay scheme for ^{142}Eu decay.

FIG 3. Spectrum of A=142 γ rays in the 54% Ge detector coincident with Eu K$_\alpha$ x-rays in the HPGe detector. Background transitions from ^{142}Sm populated by the intense ^{142}Eu source produced in this experiment are indicated.

FIG 4. Decay scheme for ^{142}Gd decay.

FIG 5. Spectrum of A=142 γ rays in the 54% Ge detector coincident with Gd K$_\alpha$ x-rays in the HPGe detector.

FIG 6. Decay scheme for ^{142}Tb^g decay.

FIG 7. Spectrum of A=142 γ rays in the HPGe detector coincident with the 182- and 212-keV γ rays in the 54% Ge detector.

FIG 8. Decay schemes for ^{140}Eu^m, ^{142}Tb^m and ^{142}Dy decays.

FIG 9. Spectrum of A=140 γ rays in the 54% Ge detector coincident with Sm K$_\alpha$ x-rays in the HPGe detector.

FIG 10. Decay scheme for ^{140}Eu^g decay.

FIG 11. Decay curve for the 185.3-keV γ-ray from ^{140}Eu^m decay.

FIG 12. Spectrum of A=140 γ rays in the 54% Ge detector coincident with Eu K$_\alpha$ x-rays in the HPGe detector.

FIG 13. Decay scheme for ^{140}Gd decay.

FIG 14. Spectrum of A=140 γ rays in the 54% Ge detector coincident with Gd K$_\alpha$ x-rays in the HPGe detector.

FIG 15. Decay scheme for ^{140}Tb decay.

FIG 16. Ground-state $0^+\rightarrow1^+$ logft values for even-even nuclei with Z=60-70 and N=74-86. (a) Experimental logft values (Reference 38) (b) Predicted logft values from shell model calculations (Reference 39).

FIG 17. Experimental $1^+\rightarrow0^+$ ground-state logft values.

0 10 20 30 40 50

mm

500 μm Be

n-Ge
64.9 φ x 57.8 mm
$\eta_{Co} = 52.3\%$
$\Omega_X = 28.1\%$

n-Ge
51.6 φ x 55.3 mm
$\eta_{Co} = 24.3\%$
$\Omega_X = 3.2\%$

500 μm Be

1 mm Pilot F, 38.2 mm φ

250 μm Be

50 μm Mylar Tape

13.8 μm Si, 50 mm^2

718 μm Si, 200 mm^2

50 μm Be

250 μm Be

HPGe

38 φ x 12.5 mm
$\Omega_p = 12.7\%, \Omega_X = 13.8\%$

2.34 s

1+   0.0

$^{142}_{63}$Eu

Q_{EC}=7000

(0+)   3187.9   0.24% 5.4

(0+)   3031.9   0.50% 5.1

(0+)   2522.2   1.57% 4.9
(0+)   2439.4   1.29% 5.0
(2+)   2373.9   0.77% 5.3
(2+)   2353.7   0.53% 5.4
0+   2173.6   0.41% 5.6
2+   2055.6   1.61% 5.1

(2+)   1657.9   2.74% 5.0

(0+)   1451.1   0.6% 5.7

2+   768.1   3.7% 5.2

0+   0.0   86.1% 4.1

2419.7 (2.4)
2263.7 (4.9)
1754.1 (14.6)
864.4 (0.84)
1671.3 (12.6)
2373.9 (7.5)
2353.7 (5.2)
1405.4 (4.0)
2055.8 (4.4)
1287.4 (11.4)
1657.9 (17.2)
889.8 (10.4)
1451.1 (~2) E0
683.0 (4.1)
768.1 (100)

$^{142}_{62}$Sm

Counts

Energy (keV)

Eu K x-ray Gate

70.2 s

0+ 0.0

$^{142}_{64}$Gd

$Q_{EC}=4200$

2160.9 0.22% 6.0

2025.6 0.7% 5.6
1956.6 0.8% 5.6
1948.6 1.0% 5.5

1+   1779.1 6.3% 4.8

1485.9 0.11% 6.7
1480.9 0.34% 6.2
1+   1438.4 7.1% 4.9
1+   1412.9 3.19% 5.2
1383.3 0.45% 6.1

1000.2 1.79% 5.7
935.6 0.93% 6.0
750.2 1.7% 5.8
732.5 1.34% 6.0
704.9 0.88% 6.1
660.9 0.77% 6.2
631.7 1.56% 5.9
619.7 1.89% 5.9
614.6 0.8% 6.2
591.3 1.30% 6.0
585.7 0.94% 6.2
550.6 0.38% 6.6
544.4 0.52% 6.5
526.2 6.35% 5.4
503.0 1.82% 5.9
496.6 0.35% 6.7

284.4 3.7% 5.7
280.2 1.47% 6.1

(2)-   178.9

1+   0.0 52.1% 4.7

$^{142}_{63}$Eu

1982 (~2)
1846.7 (6)
1956.6 (7)
1948.6 (9)
1779.1 (22.1)
1599.7 (18)
1495.0 (5.9)
1275 (~2)
1187 (~6)
1158 (~2)
1307 (~1)
1302 (~3)
1438.4 (11)
1259.6 (38.2)
853 (~1)
823.9 (21)
1412.4 (6.8)
1233.9 (15.0)
1133 (1.3)
910.0 (2.4)
862 (~3)
1204.4 (4)
1000.2 (14)
821 (~2)
935.6 (4.4)
651.3 (2.9)
203 (~0.8)
750.2 (7.2)
572 (5)
472 (~1)
247.2 (1.60)
732.4 (5.1)
553 (~3)
448.2 (1.8)
228 (~0.9)
704.9 (7.9)
660.9 (4.3)
482.0 (2.6)
631.7 (9.5)
136 (~1)
105 (~1)
619.7 (18.3)
336 (~0.5)
614.5 (3.0) E2
335 (2)
330.4 (2.9)
591.3 (9.8)
306.9 (7.2)
585.7 (4.7)
407.0 (4.8)
550.6 (6.4)
526.2 (4.1)
526.2 (52.7) E2
347.6 (4.0)
241.7 (1.5) M1
503.0 (6.4)
222.8 (14.4) M1+E2
496.6 (~0.5)
216 (~2)
212.2 (1.53)
284.4 (55.0) M1
280.3 (33.9) E2
101.4 (0.92)
178.9 (100.0) E1

Gd K x-ray Gate

597 ms

1+   0.0

$^{142}_{65}$Tb

Q_{EC}=10400

2343.6 (1.0)
1828.7 (2.7)
1364.1 (0.8)
898.4 (1.1)
1764.1 (0.9)
1299.6 (1.6)
1799 (~2)
1587.4 (1.4)
1915.0 (2.3)
1399.2 (9.6)
934
464.9 (2)
853.1 (9.7)
388.8 (0.90)
693.7 (4.0) E2
980.1 (1.8) (E2)
465.0 (11) (E2)
515.3 (100) E2

2343.9   1.39% 5.6
2279.6   0.62% 6.0
2314.4   0.50% 6.1
2102.8   0.35% 6.3
1914.71   2.96% 5.4
1445.1   <0.5% >6.3
1368.68   2.64% 5.6
1209.12
980.05   1.9% 5.8
515.42   14.9% 5.0
0.0   73.5% 4.5

4+
(2+)
2+
0+

$^{142}_{64}$Gd

Sm K x-ray Gate

1.51 s

1+   0.0

$^{140}_{63}$Eu

Q_{EC}=8400

Level		Energy	Feeding	log ft
(0+)		2482.4	1.07%	5.4
(2+)		2289.9	0.26%	6.1
(2+)		2284.1	1.30%	5.4
(0+)		1933.2	0.26%	6.3
(0+)		1628.6	0.58%	6.0
(2+)		1599.1	3.5%	5.2
(2+)		1420.3	0.35%	6.3
4+		1246.5		
(0+)		990.7	1.6%	5.8
2+		530.94	21%	4.8
0+		0.0	70%	4.4

1952.0 (1.4)
1491.3 (2.1)
882.7 (0.2)
2289.1 (0.2)
1758.7 (0.4)
1299.4 (0.3)
2283.9 (0.5)
1752.8 (1.9)
1293.6 (1.2)
685.1 (0.9)
1402.2 (0.9)
1097.7 (2.0)
1068.0 (11.0)
608.6 (1.9)
352.4 (0.4)
1420.3 (1.2)
715.4 (0.6)
459.9 (11.0)
531.0 (100)

$^{140}_{62}$Sm

15.8 s

0+   0.0

$^{140}_{64}$Gd

Q_{EC}=4800

1041.4 (13)

1131.1 (5.1)

918 (9)

903.2 (3.2)

708.1 (9.5)

749.9 (100)

575.4 (39) M1

558.7 (33)

296.6 (12.7) M1

722.3 (27)

304.5 (1.3)

269.0 (1.9)

495.8 (9.5)

436.4 (7.0)

546.5 (20.3)

372.0 (3.8)

344.5 (1.9)

313.5 (12.0)

453.4 (19)

278.4 (10.1)

261.8 (7.6) M1

446.9 (6.3)

272.4 (10.8)

427.9 (11.4)

253.3 (8.9)

236.7 (8.9)

417.7 (39)

379.0 (54)

186.7 (3.8)

191.2 (49)

185.3 (10) (E2)

174.8 (108) M1

1215.99   1.4%   5.3

1131.1   0.56%   5.8

1092.6   1.0%   5.5

1077.8   0.35%   6.0

882.69   1.05%   5.6

749.93   20.8%   4.4

722.28   3.4%   5.2

687.04   1.08%   5.7

610.99   0.80%   5.9

546.55   2.7%   5.4

535.7   0.22%   6.5

488.1   1.4%   5.7

453.28   2.6%   5.4

446.98   2.1%   5.5

427.93   3.6%   5.3

417.72   4.4%   5.2

379.0   6.2%   5.1

361.3   0.56%   6.1

191.24

185.29

174.59

1+

3+

2+

1+   0.0   46%   4.4

$^{140}_{63}$Eu

2.4 s

(5)   0.0

$^{140}_{65}$Tb

Q_{EC}=>11300

627.8 (52)

6+   1456   <50%>5.0

508 (~100)

4+   837   <50%>5.1

328.4 (100)

2+   328.4

0+   0.0

$^{140}_{64}$Gd

2.3 s

0+   0.0

$^{142}_{66}$Dy

Q_{EC}=7100

<59 (E3)
<48 (M2)

98.3 (0.12) (E3)
68.5 (1.8) M2

5-   280.2   303 ms

.5-   ≤234   125 ms

185.3 (92) E2
10.7 (M1)
174.8 (100) M1

211.6 (100)
29.7 (0.32) M1+E2
181.9 (12.3)

3+   185.3

2+   174.6

3+   211.60

2+   181.90

1+   0.0

1+   0.0   94%4.1

$^{140}_{63}$Eu

$^{142}_{65}$Tb

$0^+ \longrightarrow 1^+$

(a)

N=78
N=76
N=80
N=74

N=86
N=84
N=82

SHELL MODEL

$\pi d_{5/2} \longrightarrow \nu d_{3/2}$

$\pi h_{11/2} \longrightarrow \nu h_{9/2}$
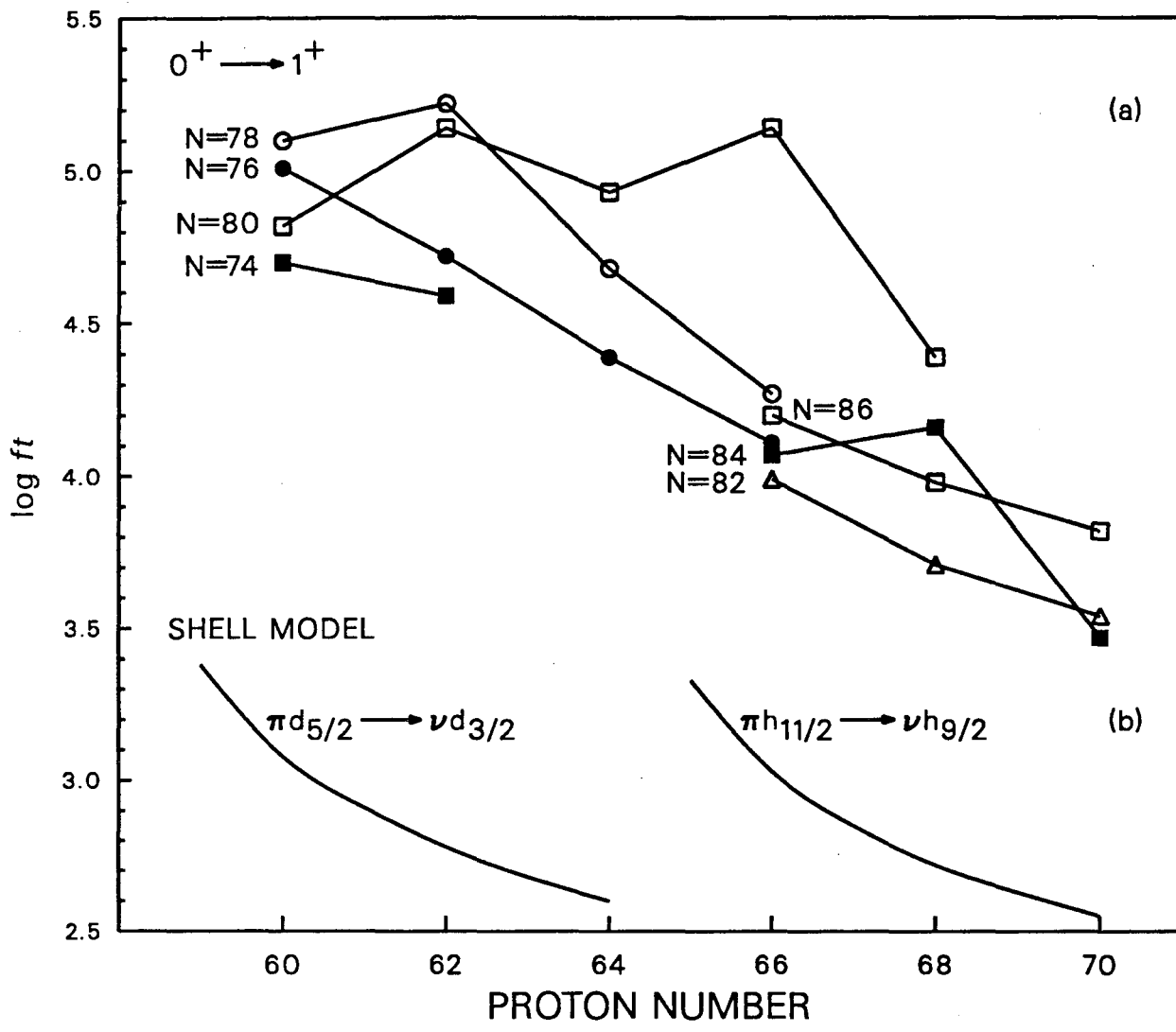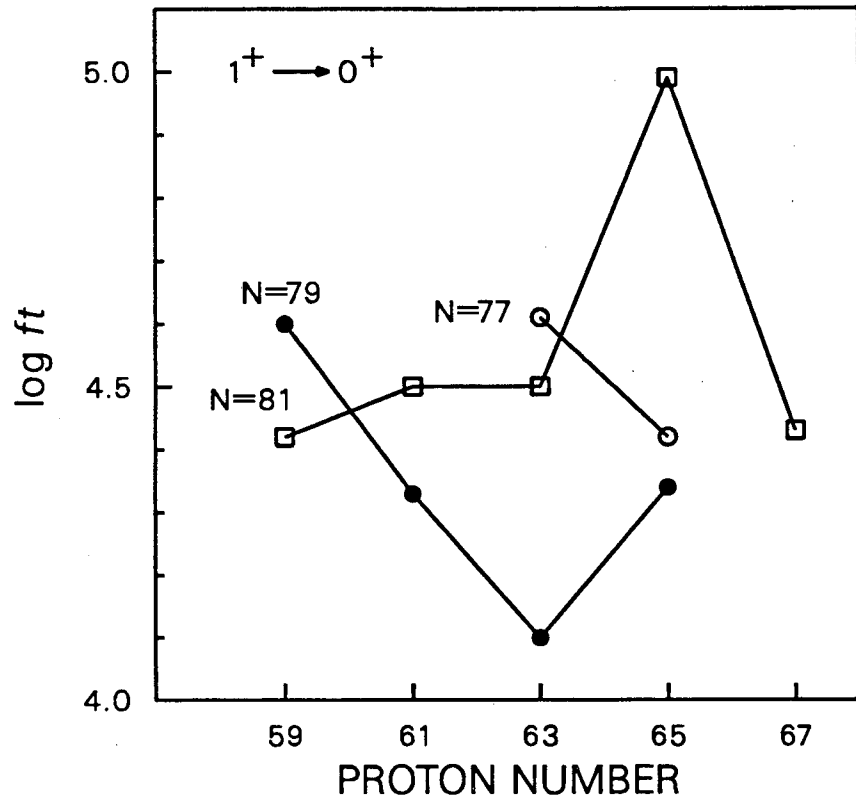
(b)

$\log ft$

PROTON NUMBER

LAWRENCE BERKELEY LABORATORY
UNIVERSITY OF CALIFORNIA
INFORMATION RESOURCES DEPARTMENT
BERKELEY, CALIFORNIA 94720